Vibration Suppression and Disturbance Rejection Control on Torsional Systems

Yoichi Hori

Department of Electrical Engineering, University of Tokyo,
7-3-1 Hongo, Bunkyo, Tokyo 113, JAPAN
Fax: +81(3)5800-3865, E-mail: hori@kaya.t.u-tokyo.ac.jp

Abstract: Vibration suppression and disturbance rejection in torsional systems are important issue in the future motion control. For example, in recent steel rolling mill systems, according to the application of high response AC drive system, the long shaft between the motor and the roll can no longer be assumed stiff. In this paper, first, I review various control strategies proposed until now: simple acceleration feedback, model following control, state feedback and so on. Next, I propose two new control techniques based on the disturbance observer. One is the "resonance ratio control" based on the "fast disturbance observer". Another is the "slow disturbance observer". In both cases, by realizing Manabe's model polynomial, the 2-inertia non-stiff system can be controlled effectively.

Keywords: vibration suppression, disturbance rejection, torsional system, robust control, disturbance observer, polynomial approach

1. INTRODUCTION

Vibration suppression and disturbance rejection in flexible system must be important in the future motion control. It originates in the steel rolling mill system, where the load is coupled to the driving motor by a long shaft. As the newly required speed response is very close to the first resonant frequency of such systems, only the conventional techniques based on P&I control are not effective enough.

To overcome the problems, various control strategies have been proposed mainly for controlling the 2-inertia system, the simplest model of the flexible system.[1][2] Here, we can see the history of control theory: simple acceleration feedback, model following control, observer-based state feedback, and modern H control. In this paper, I will give a brief review of these methods, except for H control methods, because we can see a lot of reviews on H control application.

Instead, I will propose and compare two relatively simple and practical control techniques based on the disturbance observer. One is the "resonance ratio control" based on the "fast disturbance observer". Resonance ratio, the ratio of the resonance and anti-resonance frequencies in 2-inertia system, plays an important role. By feeding back the torsional torque estimated by the "fast disturbance observer", the virtual motor inertia moment can be changed to any arbitrarily value. This means that we can change the resonance frequency and the resonance ratio. Yuki suggested that vibration can be suppressed effectively by adjusting the resonance ratio to be about $\sqrt{5}$.[13] I will show that $0.8\sqrt{5}$ is the optimal ratio in the speed control of the 2-inertia system by realizing Manabe's model polynomial.

Another method is the application of "slow disturbance observer" originally proposed by Umida.[15] In both cases, by realizing "Manabe's model polynomial", the 2-inertia system can be controlled effectively.

2. STEEL ROLLING MILL SYSTEM and its MATHEMATICAL MODEL

The problem originates in the steel rolling mill system, where the load is coupled to the driving motor by a long shaft.[3][4] The small elasticity of the shaft gets magnified and has a vibrational effect on the load speed.

Our aim is to control the roll speed in the presence of
   (1) torsional vibration,
   (2) system parameter variation,
   (3) disturbance torque T_L,
and (4) in the absence of a dedicated loadside speed sensor.

P&I controller used until now was designed to control one-inertia system, where the coupling shafts are assumed to have infinite stiffness, but the new requirements as follows force us to develop new techniques.

   (1) faster speed response,
   (2) rejection of disturbance on the loadside,
and (3) robustness to parameter variations.

As the newly required response speed is very close to the resonant frequency of the system. It has been shown that there is a limit to which the proportional gain of the P&I controller can be raised to improve performance. The conventional P&I controller is not effective enough and falls short of the new requirements.

The problem is not restricted anymore to the case of rolling mills.[5] New areas such as robotic flexible joint, large scale space structure and very precise positioning system have the same problem. Parameter variation is a very much existent phenomenon in these areas. Space structures are multi-inertia systems with long coupling lengths, but a research in 2-inertia systems is still a well justified starting point.

We can find numerous papers which dealt with a multi-inertia system (in most cases, 2-inertia systems are assumed), and also a few review papers to compare some of them are reported. A spring-coupled 2-inertia system has been investigated as the benchmark problem in ACC'90 and '91.[6] In SICE, Japan, similar bench mark problems are presented and several techniques are proposed and discussed.[7] One of the important points to notice is that we should consider not only the resonant frequency but also the wide range of the inertia ratio given by $R_0 = J_L$ (load inertia)$/J_{M0}$(motor inertia). It is not easy to develop a general method applicable to a wide range of R_0.

Fig.1 illustrates the typical configuration of steel rolling mill system. This system is basically the distributed parameter system. By using the modal analysis, it can be modeled as a multi-inertia (for example, 12 inertia moments) system having several inertia moments and springs.
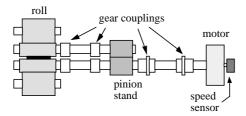
Fig.1 Typical configuration of steel rolling mill system.
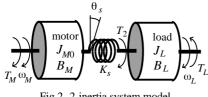

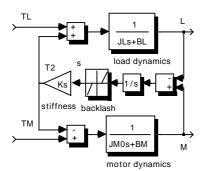Fig.2 2-inertia system model.

Fig.3 Block diagram of 2-inertia system.

The 2-inertia model shown in Fig.2 is the simplest model considering up to the first model of the multi-inertia system. It should be reminded that the 2-inertia model has a big modeling error. Fig.3 shows the block diagram of the 2-inertia system.[1][2] Its state equations take the form of

$$
\begin{pmatrix} \dot{\omega}_M \\ \dot{\theta}_s \\ \dot{\omega}_L \end{pmatrix} = \begin{pmatrix} \dfrac{-B_M}{J_{M0}} & \dfrac{-K_s}{J_{M0}} & 0 \\ 1 & 0 & -1 \\ 0 & \dfrac{K_s}{J_L} & \dfrac{-B_L}{J_L} \end{pmatrix} \begin{pmatrix} \omega_M \\ \theta_s \\ \omega_L \end{pmatrix} + \begin{pmatrix} \dfrac{1}{J_{M0}} \\ 0 \\ 0 \end{pmatrix} T_M + \begin{pmatrix} 0 \\ 0 \\ \dfrac{1}{J_L} \end{pmatrix} T_L \tag{1}
$$

The state variables are ω_M, θ_s and ω_L. The control input is the motor torque T_M. The output variable we can measure is the motor speed ω_M. The controlled variable is the load speed ω_L and the disturbance T_L is injected directly into the loadside.

The transfer function matrix between the input and output is given by

$$
\begin{pmatrix} \omega_M \\ \omega_L \end{pmatrix} = \begin{pmatrix} G_{11}(s) & G_{12}(s) \\ G_{21}(s) & G_{22}(s) \end{pmatrix} \begin{pmatrix} T_M \\ T_L \end{pmatrix} \tag{2}
$$

$G_{11}(s)$, the transfer function from T_M to ω_M, which is important for the closed loop design is given by

$$
\begin{aligned}
G_{11}(s) &= \frac{J_L s^2 + B_L s + K_s}{J_{M0}J_L s^3 + (J_{M0}B_L + J_L B_L)s^2 + \{K_s(J_{M0}+J_L) + B_M B_L\}s + K_s(B_M+B_L)} \\
&\simeq \frac{1}{s}\frac{J_L s^2 + K_s}{J_{M0}J_L s^2 + K_s(J_{M0}+J_L)} = \frac{1}{J_{M0}s}\frac{s^2+\omega_a^2}{s^2+\omega_{r0}^2}
\end{aligned} \tag{3}
$$

The Bode diagram of this transfer function is drawn in Fig.4. The resonant and anti-resonant frequencies are given by

$$
\omega_{r0} = \sqrt{\frac{K_s}{J_L}\left(1+\frac{J_L}{J_{M0}}\right)} \tag{4}
$$

and

$$
\omega_a = \sqrt{\frac{K_s}{J_L}} \tag{5}
$$

At these frequencies, the phase characteristics change drastically. The resonance ratio, which plays an important role, is defined by eq.(6).

$$
H_0 = \frac{\omega_{r0}}{\omega_a} = \sqrt{1+\frac{J_L}{J_{M0}}} = \sqrt{1+R_0} \tag{6}
$$

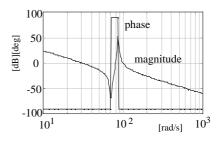where R_0 is called the inertia ratio given by $R_0 = J_L/J_{M0}$.

Fig.4 Bode plot of the transfer function from T_M to ω_M.
(J_{M0}=0.02, J_L=0.01[kgm^2], B_M=B_L=0, K_s=50[Nm/rad])

3. VARIOUS CONTROL STRATEGIES

3.1 P&I Speed Controller

Fig.5 shows the simulation result of P&I controller which is designed for 1-inertia system where the stiffness of the shaft is infinite. The response is vibrating and the effect of the disturbance torque of 50[Nm] added at t=0.5[s] is vibrational and very large.
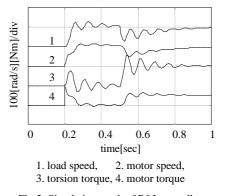

1. load speed,   2. motor speed,
3. torsion torque, 4. motor torque

Fig.5 Simulation result of P&I controller.
(J_{M0}=0.02, J_L=0.01[kgm^2], B_M=B_L=0, K_s=50[Nm/rad])

3.2 Time Derivative Feedback

We need a countermeasure to cope with the vibration when the crossover frequency ω_c of the speed minor loop increased and its ratio to the mechanical resonant frequency ω_o became 2.5~3. For this aim, the so-called speed damping controller to insert a phase lead compensator into the speed feedback path was used.

The basic technique of vibration suppression control is the speed derivative feedback. In the system of Fig.6 proposed relatively recently, we can see a fairly good vibration suppression if the derivative gain K_d is adjusted appropriately.[8]
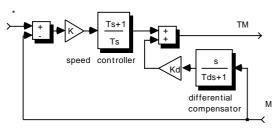
Fig.6 Speed derivative compensation system.

3.3 Model Following Controls

The controls in this category are aiming to realize similar response characteristics to that of the reference model by injecting the same input both to the reference model and the real plant and by feeding back the difference of their output signals. SFC is the representative control in this category.

<Simulator Following Control>

Simulator Following Control (SFC), proposed by Kurosawa, is an excellent practical method to suppress the effect of parameter variation and the torsional vibration.[9] It is widely used in actual industrial drive systems like rolling mill or elevator system. Fig.7 shows its block diagram. The difference between the output of the motor model and the actual motor speed is added to the torque command.

One of the advantages of SFC is that SFC is the optional function and that SFC gain can be easily adjusted on site. However, it is unclear how to get better performance than that in Fig.7. Recently, the disturbance observer based method is proved to be equivalent to SFC. The observer technique is superior for further performance improvement.

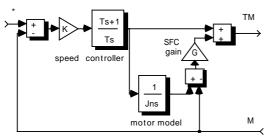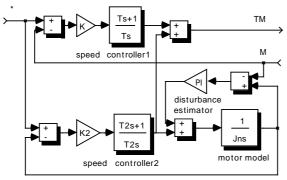

Fig.7 Simulator following control system.

Fig.8 Model following TDOF control system.

<Model Following TDOF Control>

Fig.8 shows the model following TDOF (Two-Degree-Of-Freedom) control system proposed by Koyama.[10] Speed controller 1 is the low gain controller only to stabilize the plant. The main controller is controller 2, which controls the model with no vibrational

components. The control input of controller 2 is also used for the real plant. The difference between the real plant output and the model output is fed back via P&I controller called disturbance estimator.

3.4 Application of Disturbance Observer

Disturbance observer was originally developed for disturbance rejection and robustification to parameter variations in 1-inertia system.[11][12] If we apply this technique to the 2-inertia system as it is, the free vibration due to the load inertia and the spring is induced because the torsional torque T_2 is almost completely compensated for.

Disturbance observer has three parameters: the compensation gain, the cut-off frequency of observer, and the inertia moment to be used in the observer. It is pointed out that, by appropriately selecting these parameters, vibration can be effectively suppressed in 2-inertia system.

<Resonance control>

Yuki proposed the resonance control which uses the fast disturbance observer.[13] By feeding back 1-K of the estimated disturbance, the original 2-inertia system is changed to a new system, where the motor inertia is changed to 1/K times of the real inertia: $J_M = J_{M0}/K$.

That means the resonant frequency of the new system is changed to

$$\omega_r = \sqrt{\frac{K_s}{J_L}\left(1 + \frac{J_L}{J_{M0}}K\right)} \tag{7}$$

and the resonance ratio can be controlled by K as

$$H = \frac{\omega_r}{\omega_a} = \sqrt{1 + \frac{J_L}{J_{M0}}K} \tag{8}$$

He called this technique "resonance control". The anti-resonant frequency does not change. Yuki suggested that $R=\sqrt{5}$ ($J_M=J_L/4$) is the optimal ratio for effective vibration suppression in a flexible robotic arm controlled by a P&D controller. This optimal resonance ratio is also applied to the speed control system with a P&I controller. It corresponds to the pole allocation of the closed system at the quadruple pole.[14]

It should be noted that, when the motor inertia is much larger than the load inertia as in the steel rolling mill system, the resonance ratio control of $R=\sqrt{5}$ makes the disturbance response poorer. For example, when we realize $R=\sqrt{5}$ for the system with $J_{M0}>J_L/4$, $K>1$ is needed. This means that the estimated disturbance is used to increase its effect. This fact suggests that the vibration suppression and the disturbance rejection are opposite objectives.
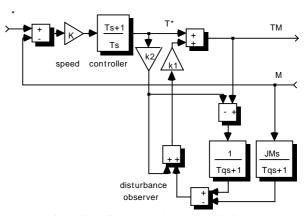
<Slow Disturbance Observer>

Fig.9 Slow disturbance observer application.

Fig.9 shows the original form of the slow disturbance observer

proposed by Umida.[15] The configuration with two gains (k_1 and k_2) seems complicated, but it is basically a simple disturbance observer in 1-inertia system.

For simplicity, putting as k_1=1, k_2=0, eq.(9) is obtained

$$\omega_M = \frac{1}{J_{M0}s} \left(\frac{s+\omega_q}{s + \frac{J_L}{J_{M0}}\omega_q} T_M^* - \frac{s}{s + \frac{J_L}{J_{M0}}\omega_q} T_2 \right) \qquad (9)$$

where $\omega_q = 1/T_q$. We can see that the phase lead compensation from torque command and the derivative feedback from the torsional torque are applied. By analyzing the transfer characteristics from T_M to θ_s, Iwata showed that the optimal observer's cut-off frequency is given by

$$\omega_q = \sqrt{\frac{2}{R_0^2 + 1}} \, \omega_a \qquad (10)$$

which is a little smaller than the anti-resonant frequency.[16]

3.5 State Feedback Controls

Various state feedback techniques to locate the system poles to desired positions have been investigated.[17][18] In 2-inertia system case, as only the motor torque (or current) and the motor speed are measurable, we should estimate other state variables by using an state observer. When our aim is limited only to the vibration suppression, the disturbance torque T_L can be neglected in the observer design. In contrast, when we need quick disturbance rejection performance, we should design a disturbance observer together with the state observer.

<SFLAC>

SFLAC (State Feedback and Load Acceleration Control) is proposed by Hori, et.al.[17] The observer estimates the unmeasurable state variables: ω_L and θ_s, and the disturbance T_L simultaneously. The extended system is made by adding the disturbance equation: $\dot{T}_L$=0. Minimal order observer is designed and the observer poles are assigned at $s=-\omega_g$. By using the three state variables: the measured value ω_M and the estimates of $\hat{\omega}_2$ and $\hat{\theta}_s$, the state feedback

$$T_M = T_M^* + f_1\omega_M + f_2\hat{\omega}_L + f_3\hat{\theta}_s \qquad (11)$$

is applied to allocate the system poles at $s=-\omega_f$.

Next, by assuming the output of the speed controller as the load acceleration command, the torque reference is given as

$$T_M^* = K_a \left\{ K \frac{Ts+1}{Ts} (\omega^* - \omega_M) - \hat{\omega}_L \right\} \qquad (12)$$

to control the load acceleration. The load acceleration $\hat{\omega}_L$ can be estimated as

$$\hat{\omega}_L = \frac{K_{sn}}{J_{2n}} \hat{\theta}_s - \frac{1}{J_{Ln}} \hat{T}_L \qquad (13)$$

Fig.10 illustrates the block diagram of SFLAC. Fig.11 shows its excellent time response characteristics with the +/-100[Nm] torque limiter. SFLAC seems to have a very complex structure, but its design concept is straightforward and clear.
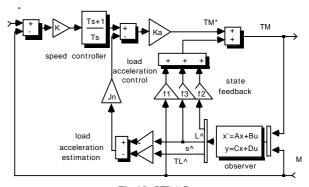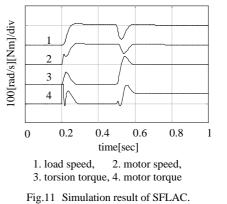

Fig.10 SFLAC.
(State Feedback and Load Acceleration Control)

1. load speed, 2. motor speed,
3. torsion torque, 4. motor torque

Fig.11 Simulation result of SFLAC.
(J_{M0}=0.02, J_L=0.01[kgm^2], B_M=B_L=0, K_s=50[Nm/rad])

<Suppression of Higher Order Vibration Modes>

Fig.12 shows the latest proposal of Kubo and Dhaouadi.[18] The distinct feature of Fig.12 is that two observers are used. The torsional torque observer is the first order disturbance observer with quick convergence. The two inertia observer is similar to one in SFLAC but has slower convergence speed so as not to be affected by the higher order vibrational modes. The difference between the disturbance torques estimated by these two observers involves higher order vibration modes' effect and equivalent torques caused by various nonlinear characteristics. By feeding back this signal, the suppression of higher order vibration modes and the effect of backlash is possible. This method is a straightforward application of observer and state feedback technology and its control performance is very excellent.
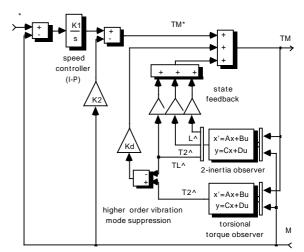

Fig.12 Higher order vibration mode suppression
control using two observers.

3.6 Future Direction of the Torsional System Control

In the near future, sophisticated H   controllers will be applied to torsional system control. In the past, the author thought that H controllers should be designed very easily without any deep consideration, but it was wrong. H   controller design needs highly sophisticated skill. Much knowledge is needed in selecting the signals and the weighting functions.

Recently, μ-synthesis is applied and shows good results.   In particular, Hirata modeled the parameter variation in 2-inertia system using descriptor form representation and applied μ-synthesis. New techniques are being developed which deal with the real number parameter variations as they are. At present, it is easy just to design excellent controllers on computer. However, we should take some practical requirements into account. For example,

  (1) Anyone should understand the new technique.
       (Complicated theory is never used widely.)
  (2) Operator should adjust the controller on site easily.
       (We can not convey CAD into factory.)
  (3) Controller should be simple.
       (Process computer is busy for doing many other jobs
        than control algorithms.)
  (4) Control system should be robust to backlash and
     torque limit.
       (Controller should be adjusted quickly according to
        the practical restriction.)

It is not easy to combine H   controller with adaptive techniques. Recently, I proposed very simple methods mainly based on the conventional polynomial approach, where the controller's order is only 2. I will like to explain these methods in the next chapter. Its control performance is better than or equivalent to any other methods reviewed here. Such a conventional technique without using the latest frequency-shaping technique is also attractive.

4. TWO NOVEL TECHNIQUES using DISTURBANCE OBSERVER

4.1 System Model

In Fig.3, the block diagram of the 2-inertia system, I put

$$J_{M0} + J_L = 1 , \quad K_s = 1 \qquad (14), (15)$$

These equations mean that the total inertia moment of the motor and the load, and the spring coefficient are fixed. Various 2-inertia systems with different inertia ratios will be considered under these relations.

Fig.13 illustrates the transfer function block diagrams neglecting the disturbance T_L. Fig.13(a) has a redundancy because we can see a pole-zero cancellation. Representation of Fig.13(b) is based on the coprime factorization.
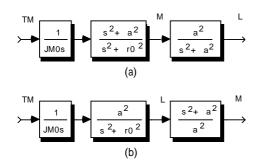

(a)

(b)

Fig.13 Transfer function representations.

4.2 Resonance Ratio Control by Fast Disturbance Observer

<Resonance Ratio Control>

Fig.14 depicts the resonance ratio control using the fast disturbance observer. In usual disturbance observer applications, 100% of the estimated disturbance is fed back to the motor torque. In contrast to this, 1-K of the estimated disturbance is fed back. Fig.15 shows the new system where the resonance ratio control is applied. We can change the virtual motor inertia moment to any value as given by

$$J_M = J_{M0}/K \qquad (16)$$

This means that we can change the resonant frequency as

$$\omega_r = \sqrt{ K_s \left(\frac{1}{J_M} + \frac{1}{J_L} \right) } \qquad (17)$$

and the resonance ratio as

$$H = \sqrt{1+R} = \sqrt{1 + \frac{J_L}{J_M}}$$
$$= \sqrt{1 + \frac{J_L}{J_{M0}/K}} = \sqrt{1+R_0 K} \qquad (18)$$
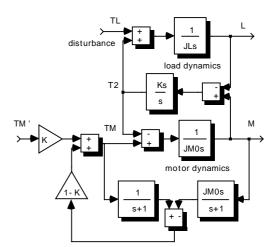
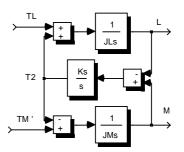

Fig.14 Block diagram of the resonance control.

Fig.15 The effect of the resonance ratio control.

From eq.(18), we can calculate K which realizes the optimal resonance ratio H.

$$K = \frac{H^2 - 1}{R_0} \qquad (19)$$

<Normalization>

Fig.16 is the block diagram from the new input torque T_M' to the motor speed ω_M. For simplicity, I normalized the system using $\omega_a(=1)$ and $J_L(=1)$ as is shown in Fig.17.
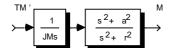
Fig.16 Block diagram from $T_M{}'$ to ω_M.

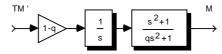

Fig.17 Normalized system by putting $\omega_a=1$ and $J_L=1$.

Relations among some variables are summarized as follows.

$$\omega_r=\sqrt{1+R}\ \omega_a=H\omega_a,\ \ H=\sqrt{1+R}=1/\sqrt{q} \qquad (20),(21)$$

$$q=\frac{1}{H^2}=\frac{1}{1+R}<1 \qquad (22)$$

$$\frac{J_L}{J_M}=R=H^2-1=\frac{1}{q}-1 \qquad (23)$$

$$\frac{J_M}{J_L}=\frac{1}{R}=\frac{1}{H^2-1}=\frac{q}{1-q} \qquad (24)$$

<Controller Design using Manabe Polynomials>

Using the speed controller $C(s)$, P, P&I and PID controllers are designed one by one considering the closed loop characteristics. (See Fig.18.)
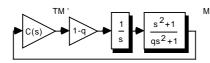

Fig.18 Design of the speed controller $C(s)$.

P Controller

In the case of $C(s)=K_p$, the characteristic equation of the closed loop system takes the form of

$$\begin{aligned}P(s)&=s(1+qs^2)+K_p(1-q)(1+s^2)\\ &=qs^3+K_p(1-q)s^2+s+K_p(1-q)\\ &=a_3s^3+a_2s^2+a_1s+a_0\end{aligned} \qquad (25)$$

My technique is to make the above characteristic equation to an appropriate "good" polynomial. Many "good" polynomials have been proposed.[19][20] For example, the relationship of Manabe Polynomial[21] is given by

$$\tau=\frac{a_1}{a_0}=\frac{1}{K_p(1-q)} \qquad (26)$$

$$\gamma_1=\frac{a_1^2}{a_0\,a_2}=\frac{1}{K_p^2(1-q)^2}=2.5 \qquad (27)$$

$$\gamma_2=\frac{a_2^2}{a_1\,a_3}=\frac{K_p^2(1-q)^2}{q}=2 \qquad (28)$$

τ defined by eq.(26) as the ration of a_1 to a_0 is called the equivalent time constant. γ_i ($i=1,2,...$) is the index which represents "goodness" of the polynomial. Manabe recommends the polynomials satisfying $\gamma_1=2.5$ and $\gamma_i=2$ ($i=2,3,....$). By solving eqs.(26)-(28) with respect to τ, q and K_p, we easily obtain

$$q=\frac{1}{5},\ \ H=\sqrt{5},\ \ R=4,\ J_M{:}J_L=1{:}4 \qquad (29)$$

This means that 1:4 is the best inertia ratio for vibration suppression. The best ratio is realized by the resonance ratio control. The normalized controller constants are given by

$$\tau=\frac{\sqrt{10}}{2},\ \ K_p=\frac{\sqrt{10}}{4} \qquad (30),(31)$$

The actual controller constants are then given by

$$\tau=\frac{\sqrt{10}}{2}\frac{1}{\omega_a},\ \ K_p=\frac{\sqrt{10}}{4}J_L\omega_a \qquad (30'),(31')$$

P&I Controller

When we use P&I controller given by $C(s)=K_p+K_I/s$, the characteristic equation is

$$\begin{aligned}P(s)&=s^2(1+qs^2)+(K_ps+K_I)(1-q)(1+s^2)\\ &=qs^4+K_p(1-q)s^3+\{1+K_I(1-q)\}s^2\\ &\qquad +K_p(1-q)s+K_I(1-q)\\ &=a_4s^4+a_3s^3+a_2s^2+a_1s+a_0\end{aligned} \qquad (32)$$

The relationship of Manabe Polynomial is represented by

$$\tau=\frac{a_1}{a_0}=\frac{K_p(1-q)}{K_I(1-q)}=\frac{K_p}{K_I} \qquad (33)$$

$$\gamma_1=\frac{a_1^2}{a_0\,a_2}=\frac{\{K_p(1-q)\}^2}{\{1+K_I(1-q)\}\,K_I(1-q)}=2.5 \qquad (34)$$

$$\gamma_2=\frac{a_2^2}{a_1\,a_3}=\frac{\{1+K_I(1-q)\}^2}{\{K_p(1-q)\}^2}=2 \qquad (35)$$

$$\gamma_3=\frac{a_3^2}{a_2\,a_4}=\frac{\{K_p(1-q)\}^2}{q\{1+K_I(1-q)\}}=2 \qquad (36)$$

By solving these equations, we obtain

$$q=\frac{5}{16},\ \ H=\frac{4}{5}\sqrt{5},\ \ R=\frac{11}{5},\ \ J_M{:}J_L=5{:}11 \qquad (37)$$

Eq.(37) means that $0.8\sqrt{5}$ is the optimal resonance ratio in this case. Also, other normalized controller constants are uniquely calculated as

$$\tau=\frac{5\sqrt{2}}{2},\ \ K_p=\frac{10\sqrt{2}}{11},\ \ K_I=\frac{4}{11} \qquad (38),(39),(40)$$

The actual controller constants are given by

$$\tau=\frac{5\sqrt{2}}{2}\frac{1}{\omega_a},\ \ K_p=\frac{10\sqrt{2}}{11}J_L\omega_a \qquad (38'),(39')$$

$$K_I=\frac{4}{11}J_L\omega_a^2 \qquad (40')$$

PID Controller

When $C(s)=K_p+K_I/s+K_Ds$, the characteristic equation is given by

$$\begin{aligned}P(s)&=s^2(1+qs^2)+(K_Ds^2+K_ps+K_I)(1-q)(1+s^2)\\ &=\{q+K_D(1-q)\}s^4+K_p(1-q)s^3\\ &\qquad +\{1+K_D(1-q)+K_I(1-q)\}s^2\\ &\qquad +K_p(1-q)s+K_I(1-q)\\ &=a_4s^4+a_3s^3+a_2s^2+a_1s+a_0\end{aligned} \qquad (41)$$

The relationship of Manabe Polynomial takes the forms of

$$\tau=\frac{a_1}{a_0}=\frac{K_p(1-q)}{K_I(1-q)}=\frac{K_p}{K_I} \qquad (42)$$

$$\gamma_1=\frac{a_1^2}{a_0\,a_2}=\frac{\{K_p(1-q)\}^2}{\{1+K_D(1-q)+K_I(1-q)\}\,K_I(1-q)}=2.5 \qquad (43)$$

$$\gamma_2=\frac{a_2^2}{a_1\,a_3}=\frac{\{1+K_D(1-q)+K_I(1-q)\}^2}{\{K_p(1-q)\}^2}=2 \qquad (44)$$

$$\gamma_3 = \frac{a_3^2}{a_2\,a_4} = \frac{\{K_p\,(1\text{-}q)\}^2}{\{q+K_D(1\text{-}q)\}\{1+K_D(1\text{-}q)+K_I(1\text{-}q)\}} = 2 \qquad (45)$$

By solving these equations, the normalized controller constants are given as follows by using q as the parameter.

$$\tau = \frac{5\sqrt{2}}{2}, \quad K_p = \frac{10\sqrt{2}}{11}, \quad K_I = \frac{4}{11} \qquad (46),(47),(48)$$

$$K_D = \frac{5\text{-}16q}{11(1\text{-}q)} \qquad (49)$$

The actual controller parameters are also given by

$$\tau = \frac{5\sqrt{2}}{2}\frac{1}{\omega_a}, \quad K_p = \frac{10\sqrt{2}}{11}J_L\omega_a \qquad (46'),(47')$$

$$K_I = \frac{4}{11}J_L\omega_a^2 \qquad (48')$$

$$K_D = \frac{5\text{-}16q}{11(1\text{-}q)}J_L \qquad (49')$$

Eqs.(46)-(48) are completely same to those of P&I controller. However, the derivative gain K_D is the function of q.

This means that, whatever resonance ratio $H=1/q^2(>1)$ we choose, the optimal condition of Manabe Polynomial ($\gamma_1=2.5$, $\gamma_2=\gamma_3=...=2$) can be satisfied by the corresponding choice of K_D. It is also interesting that τ takes the same value regardless of optimal H.

When $q>5/16$, i.e., $H<0.8\sqrt{5}$, K_D should be negative. I found some reports which say that the positive feedback of acceleration is effective for vibration suppression. This corresponds to the case of $H_0<0.8\sqrt{5}$.

When we put $K_D=0$ in eq.(49), i.e., $q=5/16$, we obtain P&I controller. The resonance ratio control has a derivative function as the disturbance observer. We can notice that we do not need to use PID controller because we already implement the derivative function by using the resonance ratio control. No usage of K_D term has the advantage from the viewpoint of controller simplicity.

<Simulation Results>

Fig.19 draws the simulation block diagram and Fig.20 shows the design results of the resonance ratio control using the fast disturbance observer. Simulation is performed for three different cases, where the original systems' inertia ratios are 0.2, 1, and 5 under the condition with 10~20% model errors, backlash (+/-0.01) and torque limiter (+/-1.2).
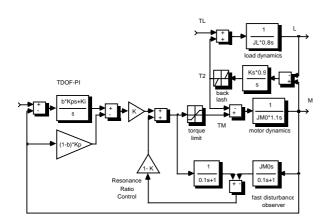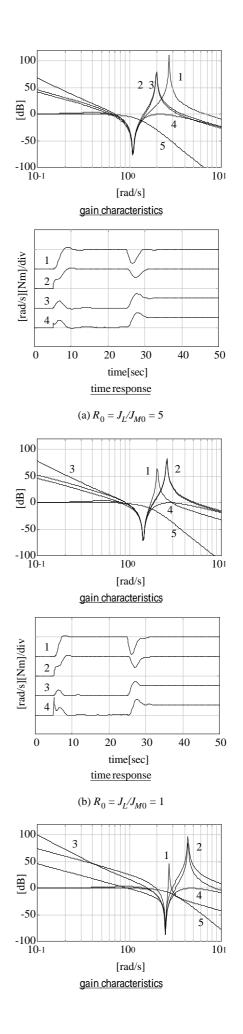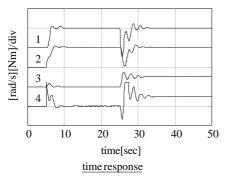

Fig.19 Simulation block diagram of the fast disturbance observer
(resonance ratio control)
with model error, backlash and torque limit.

gain characteristics

time response

(a) $R_0 = J_L/J_{M0} = 5$

gain characteristics

time response

(b) $R_0 = J_L/J_{M0} = 1$

gain characteristics

(c) $R_0 = J_L/J_{M0} = 0.2$

gain characteristics
1. ω_M/T_M ,   2. ω_M/T_M' ,   5. ω_L/ω^*
3. open loop characteristics, 4. closed loop characteristics

time response
at $t=5$, $\omega^*=1$(step); at $t=25$, $T_L=-0.5$(step)
1. load speed,   2. motor speed,
3. torsion torque,   4. motor torque

Fig.20 Simulation results (Fast Disturbance Observer).

From the various frequency characteristics plots, we can see the principle of the resonance control. In the time response simulation using SIMULINK, we can observe excellent performances both in the vibration suppression and the disturbance rejection. Moreover this method is quite effective to wide range of inertia ratio. We can see a slight performance degradation in Fig.20(c) where the inertia ratio is extremely small.

Also in Fig.20(c), we can observe that the motor torque is negative for a while just after the disturbance torque is added at $t=25$. This means that the disturbance rejection and the vibration suppression are not consistent requirements for 2-inertia systems with the smaller inertia ratio (R_0) than 11/5=2.2.

4.3 Application of Slow Disturbance Observer

<Slow Disturbance Observer>

Fig.21 shows the "slow disturbance observer" application. The disturbance observer applied to the motor side has three design parameters, i.e., the cut-off frequency ω_o , the compensation gain and the nominal inertia moment ratio r. The inertia moment used in the observer is $r\,J_{M0}$.
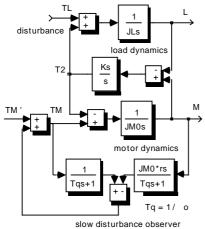

Fig.21 Application of the slow disturbance

In the "fast disturbance observer" shown in Fig.14, its cut-off frequency was high enough so that the observer's dynamics can be neglected. In contrast to this, the cut-off frequency ω_o and the inertia moment ratio r are the design parameters in the "slow disturbance observer" while its compensation gain is 1.

The "slow disturbance observer" was originally proposed by Umida[15] and was improved by Iwata.[16] Umida proposed that the optimal cut-off frequency should be a little lower than the anti-resonant frequency ω_a. Iwata gave it as the simple function of ω_a and R_0, the inertia ratio. Here, I will try to derive the optimal cut-off frequency and the other parameters simultaneously by applying Manabe's polynomial.

<Normalization>

In this case, as we can not change the motor-side inertia moment, the normalization base is only ω_a. By putting $\omega_a=1$, the 2-inertia system given by Fig.3 is normalized as Fig.22.
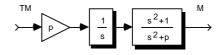

Fig.22 Normalized system by putting $\omega_a=1$.

Here, I put

$$p = H_0^2 = 1+R_0 = \frac{1}{J_{M0}} \tag{50}$$

By applying the slow disturbance observer, the transfer function from T_M', the new controlled torque input, to ω_M is given by

$$\frac{\omega_M}{T_M'} = \frac{p}{s}\,\frac{(s+\omega_o)(s^2+1)}{s\,(s^2+p)+r\,\omega_o(s^2+1)} \tag{51}$$

(See Fig.23.) Note that I use here the parameter r, the ratio of the inertia moment used in the disturbance observer to the actual motor inertia J_{M0}.

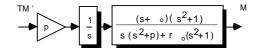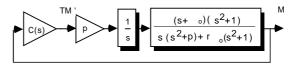Fig.23 System block diagram applied by the slow disturbance observer.

Fig.24 Design of the speed controller $C(s)$.

<Controller Design using Manabe's Polynomial>

Putting the P&I speed controller $C(s)$ as

$$K_p + \frac{K_I}{s} = K_p\,\frac{s+\omega_c}{s} \tag{52}$$

the characteristic equation of the closed loop system illustrated in Fig.24 is given by

$$\begin{aligned}
P(s) &= s^5 + (K_p p + r\,\omega_o)s^4 + \{K_p p(\omega_o+\omega_c)+p\}s^3 \\
&\quad + \{K_p p(\omega_o\omega_c+1)+r\,\omega\}s^2 + K_p p(\omega_o+\omega_c)s \\
&\quad + K_p p\,\omega_o\omega_c \\
&= a_5 s^5 + a_4 s^4 + a_3 s^3 + a_2 s^2 + a_1 s + a_0
\end{aligned} \tag{53}$$

The relationship of Manabe's Polynomial is given by the following equations.

$$\tau = \frac{a_1}{a_0} = \frac{\omega_o + \omega_c}{\omega_o \omega_c} \qquad (54)$$

$$\gamma_1 = \frac{a_1^2}{a_0\, a_2} = \frac{\{K_p p(\omega_o+\omega_c)\}^2}{\{K_p p \omega_o \omega_c\}\{K_p p(\omega_o \omega_c+1)+r\,\omega\}} = 2.5 \qquad (55)$$

$$\gamma_2 = \frac{a_2^2}{a_1\, a_3} = \frac{\{K_p p(\omega_o \omega_c+1)+r\,\omega\}^2}{\{K_p p(\omega_o+\omega_c)\}\{K_p p(\omega_o+\omega_c)+p\}} = 2 \qquad (56)$$

$$\gamma_3 = \frac{a_3^2}{a_2\, a_4} = \frac{\{K_p p(\omega_o+\omega_c)+p\}^2}{\{K_p p(\omega_o \omega_c+1)+r\,\omega_o\}\{K_p p+r\,\omega_o\}} = 2 \qquad (57)$$

$$\gamma_4 = \frac{a_4^2}{a_3\, a_5} = \frac{\{K_p p+r\,\omega_o\}^2}{\{K_p p(\omega_o+\omega_c)+p\}} = 2 \qquad (58)$$

We should find four parameters ω_o, ω_c, K_p and r which satisfy the design condition given by eqs.(55)-(58).

The procedure to solve these equations are not very easy but the results are relatively simple. First, the equivalent time constant τ is given as a constant:

$$\tau = \sqrt{25+10\sqrt{5}} \quad 6.882 \qquad (59)$$

I should omit the details, but one of the interesting results is that γ_4 is proportional to p, if other design conditions of eqs.(55)-(57) are satisfied. Regardless of the choice of r, γ_4 is given by

$$\gamma_4 = \frac{A^2}{B\,(\tau+B)}\, p \quad 0.6973\, p \qquad (60)$$

A and B are given by eqs.(63) and (64) below.

When p increases, γ_4 becomes bigger. This means that the robustness is increased. However, for systems with smaller p, γ_4 is smaller and the system becomes easily unstable. To satisfy eq.(58): $\gamma_4 = 2$ exactly, $p = 2B(\tau+B)/A^2 \sim 2.8$ should hold. This means $R_0 = 1.8$, which is very close to the easiest case also in the fast disturbance observer application.

Anyhow we can choose r as we like. Here I put $r=p$. This choice means that the disturbance observer uses the summation of motor and load inertia moments as the nominal inertia moment because

$$r\, J_{M0} = p\, J_{M0} = (1+R_0)J_{M0} = J_{M0}+J_L \qquad (61)$$

By choosing r as this, other design parameters become constants regardless of p.

I should omit the detailed derivation but the observer's cut-off frequency ω_o is finally given as the real root of the following 3rd order equation (62).

$$B\, \omega_o^3 - A\, \omega_o^2 + \tau\, \omega_o -1 = 0 \qquad (62)$$

where

$$A = \frac{-1+\sqrt{681+304\sqrt{5}}}{2} \quad 17.944 \qquad (63)$$

$$B = \sqrt{2A\,(1+A)} - \tau \quad 19.193 \qquad (64)$$

By solving eq.(62), $\omega_o = 0.3249$ is obtained. Accordingly P&I controller's parameters K_p and ω_c are given by

$$K_p = \frac{A}{B} - \omega_o \quad 0.6100 \qquad (65)$$

and

$$\omega_c = \frac{1}{B\, K_p \omega_o} \quad 0.2629 \qquad (66)$$

By multiplying ω_a, the actual ω_o and ω_c are obtained. As ω_a is the function of p (actually, $\omega_a = \sqrt{p\,/(p-1)}$), ω_o and ω_c varies according to p.

<Simulation Results>

Fig.25 illustrates the simulation block diagram. All conditions of simulation are quite same to those in the fast disturbance observer case.
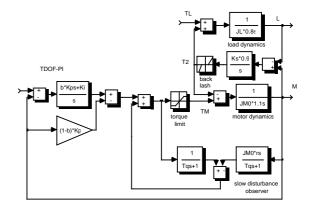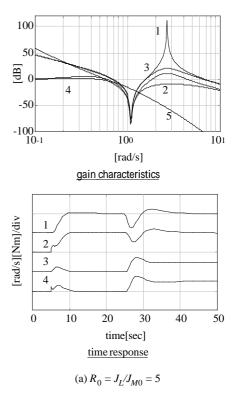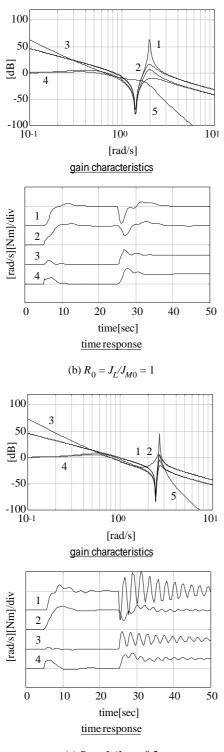

Fig.25 Simulation block diagram of the slow disturbance observer with model error, backlash and torque limit.

In Fig.26, we can see the control performances of the "slow disturbance observer". In this type, we can not see any change of the resonant frequency but big damping effect around the resonant frequency is observed. The bigger the inertia ratio, the more robust to the parameter variation and backlash because γ_4 is big enough. In systems with smaller inertia ratio, robustness is deteriorated. This is because γ_4 becomes smaller when p is smaller as is given by eq.(60). However, too big γ_4 may mean over-specification.

gain characteristics

time response

(a) $R_0 = J_L/J_{M0} = 5$

gain characteristics

time response

(b) $R_0 = J_L/J_{M0} = 1$

gain characteristics

time response

(c) $R_0 = J_L/J_{M0} = 0.2$

gain characteristics
1. ω_M/T_M ,   2. $\omega_M/T_M{}'$,   5. ω_L/ω^*
3. open loop characteristics, 4. closed loop characteristics

time response
at $t = 5$, $\omega^* = 1$(step); at $t = 25$, $T_L = -0.5$(step)
1. load speed,   2. motor speed,
3. torsion torque,   4. motor torque

Fig.26 Simulation results (Slow Disturbance Observer).

5. CONCLUSION

I reviewed some methods to deal with the vibration suppression and disturbance rejection control of torsional system. I proposed two simple but effective techniques based on the disturbance observer. One is the "fast disturbance observer" to realize "resonance ratio control", and another is the "slow disturbance observer". In both cases, I tried to realize "Manabe's Polynomial" for their characteristic equations of the closed loop system. Although the obtained controllers are of only 2nd order system, their control performance is excellent. In particular, the fast disturbance observer is superior in operation through a wide range of the inertia ratio. H controller will be also effective to this kind of vibration control, but relatively classical methods presented here are also attractive in various aspects.

REFERENCES

[1] N.Matsui and Y.Hori, "New Technologies on Motor Control", *Trans. of IEE-Japan*, Vol.113-D, No.10, pp.1122-1137, 1993.
[2] Y.Hori, "Comparison of Vibration Suppression Control Strategies in 2-Mass Systems including a Novel Two-Degrees-Of-Freedom H Controller", *IEEE 2nd International Workshop on Advanced Motion Control*, pp.409-416, 1992.
[3] T.Ohmae, et.al., "A Microprocessor-Based Motor Speed Regulator Using Fast-Response State Observer for Reduction of Torsional Vibration", *IEEE Trans. on Ind. Appl.*, Vol.23, No.5, pp.863-871, 1987.
[4] T.Harakawa, et.al., "Development of Spindle Torsional Control System using Observer for Tandem Cold Mill in Steel Production Process", *Proc. IEEE-PESC'88*, pp.106-110, 1988.
[5] U.Schaefer and G.Brandenburg, "State Position Control for Elastic Pointing and Tracking Systems with Gear Play and Coulomb Friction -A Summary of Results-", *'91 EPE*, pp.2-596 2-602, 1991.
[6] B.Wie and D.Bernstein, "A Benchmark Problem for Robust Control Design", *1990 American Control Conference (ACC'90)*, pp.961-962, 1990.
[7] S.Hara, et.al., "Benchmark Problem for Robust Control (I) and (II)", *Journal of SICE*, Vol.34, No.5, pp.403-409, No.6, pp.498-507, 1995.
[8] M.Sugano, et.al., "Torsional Vibration Suppression Control by Speed Differentiation", *IEE-Japan Technical Meeting*, SPC-90-109, 1990.
[9] T.Hasegawa, et.al., "A Microcomputer-Based Motor Drive System with Simulator Following Control", *Proc. IEEE-IECON'86*, Vol.1, p.41-, 1986.
[10] M.Koyama & M.Yano, "Two Degrees of Freedom Speed Controller using Reference System Model for Motor Drives", *'91 EPE*, 1991.
[11] K.Ohishi, et.al., "Microprocessor-controlled Dc Motor for Load-insensitive Position Servo System", *IEEE Trans. on Ind. Electron.*, Vol.34, pp.44-49, 1987.
[12] T.Umeno, T.Kaneko and Y.Hori, "Robust Servosystem Design with Two Degrees of Freedom and its Application to Novel Motion Control of Robot Manipulators", *IEEE Trans. on Ind. Electron.*, Vol.40, No.5, pp.473-485, 1993.
[13] K.Yuki, T.Murakami and K.Ohnishi, "Vibration Control of a 2 Mass system by the Resonance Ratio Control", *Trans. of IEE-Japan*, Vol.113-D, No.10, 1993.
[14] K.Sugiura and Y.Hori, "Proposal of Quad-pole Controller based on root-5 Resonance Ratio Control for 2-Mass System", *3rd International Workshop on Advanced Motion Control*, 1994.
[15] H.Umida, "Novel Control Strategies of Torsional Vibration System: A Dully Tuned Disturbance Observer", *IEE-Japan IAS Annual Meeting*, S.12-3, 1994.
[16] M.Iwata and S.Itoh, "High Performance and Adaptive Motion Control System Based on Identified Mechanical Parameter", *3rd International Workshop on Advanced Motion Control*, 1994, Berkeley.
[17] Y.Hori, H.Iseki and K.Sugiura, "Basic Consideration of Vibration Suppression and Disturbance Rejection Control of Multi-Inertia System using SFLAC (State Feedback and Load Acceleration Control)", *IEEE Transactions. on Industrial Applications*, Vol.30, No.4, pp.889-896, 1994.
[18] R.Dhaouadi, et.al., "Vibration Suppression and High Performance Speed Control of Rolling Mill Drives", *IEEE 2nd International Workshop on Advanced Motion Control*, pp.409-416, 1992.
[19] D.Graham and R.C.Lathrop, "The Synthesis of Optimum Transient Response: Criteria and Standard Forms", *AIEE Trans.*, Vol.72, pt.2, pp.273-288, 1953.
[20] V.C.Kessler, "Ein Beitrag zur Theorie Mehrschleifiger Regelungen", *Regelungstechnik*, H.8, pp.261-266, 1960.
[21] S.Manabe, "Generalization of Classical, Optimal and H Control Methods", *Journal of SICE*, Vol.30, No.10, pp.941-946, 1991.
[22] Y.Hori, "2-Mass System Control based on Resonance Ratio Control and Manabe Polynomials", *Proc. of ASCC (First Asian Control Conference)*, Vol.3, pp.III-741-744, 1994.
[23] Y.Hori, "Comparison of Torsional Vibration Controls based on the Fast and Slow Disturbance Observers", *Proc. of IPEC Yokohama '95*, 1995.